






Computer-Aided Detection of Exact Reflection and Axisymmetry in B-rep CAD Models

Mladen Buric¹ , Mario Brcic² , Nenad Bojcetic³  and Stanko Skec⁴ 

¹ University of Zagreb, mladen.buric@fsb.hr

² University of Zagreb, mario.brcic@fer.hr

³ University of Zagreb, nenad.bojcetic@fsb.hr

⁴ University of Zagreb, stanko.skec@fsb.hr

Corresponding author: Mladen Buric, mladen.buric@fsb.hr

Abstract. During Computer-Aided Design (CAD), there is often the need to check if symmetrically designed 3D CAD models indeed exhibit the intended type of symmetry. However, the symmetry information is seldom directly stored in the native CAD models and never in the neutral exchange file formats. One way to retrieve the symmetry information is the visual recognition by the expert. However, for complex geometric shapes or a significant number of CAD models from the repository, the visual recognition may be complex, time-intensive, and often only approximative. Thus, to eliminate the need for visual recognition, computer-aided symmetry detection is preferred, which deals with the automatic identification of the planes and axes of symmetry. The present study proposes a vector-based approach using face centroids to detect exact reflection and axisymmetry in 3D CAD models with Boundary Representation (B-rep). The proposed approach has been implemented in a state-of-the-art CAD system using its Application Programming Interface and tested on 150 CAD models for validation purposes. The obtained results confirmed that the proposed approach enables accurate and efficient detection of the corresponding planes and axes of symmetry.

Keywords: symmetry detection, exact symmetry, axisymmetry, reflection symmetry, Computer-Aided Design (CAD), B-rep

DOI: <https://doi.org/10.14733/cadaps.2023.884-897>

1 INTRODUCTION

Geometric symmetry (hereinafter symmetry) is often introduced into mechanical parts or assemblies as it is beneficial in terms of function [20], structural analysis [27], manufacturing [17], assembling [4], reducing complexity, or aesthetics. For example, symmetrically designed parts are less prone to assembly errors and require less assembly time [4]. Further, symmetry is used in manufacturing to define the parting planes in the stamping and molding processes [17]. In

Computer-Aided Engineering (CAE), symmetry is often exploited to reduce the size of the 3D model, consequently reducing the analysis's computational effort [27]. Moreover, in technical drawing [22], symmetrical parts may be drawn half in section and half in outside view, which reduces the number of views necessary for defining the shape of the part. At the same time, the axis of symmetry of symmetrical features does not require dimensioning, resulting in the reduction of the number of dimensions.

During Computer-Aided Design (CAD), there is often the need to check if symmetrically designed 3D CAD models indeed exhibit the intended type of symmetry. However, the symmetry information is seldom directly stored in the native CAD models and never in the neutral exchange file formats (e.g., IGS, STEP, etc.). The exceptional case when the symmetry information is stored in the native CAD model is when the geometric shape has been created by, for instance, a mirroring operation with respect to a plane. One way to retrieve the symmetry information is the visual recognition by the expert. However, visual recognition may be too difficult and time-consuming for complex geometric shapes or a significant number of 3D CAD models. In addition, exact symmetry cannot be obtained by visual recognition in any CAD model [12]. Hence, computer-aided *symmetry detection* (SD) is preferred, which deals with the automatic identification of the planes and axes of symmetry in 2D or 3D digital objects. The present study proposes an approach for detecting exact reflection and axisymmetry (see Figure 1) in 3D CAD models using the Boundary Representation (B-rep) as input.

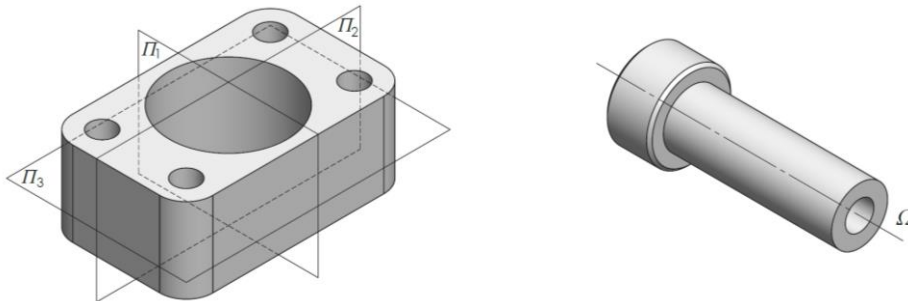


Figure 1: A mechanical part exhibiting reflection symmetry with three planes of symmetry Π_1 , Π_2 , & Π_3 (left), and an axisymmetric part with its axis of symmetry Ω (right). Reflection symmetry means that the part is invariant under mirroring about a plane, while axisymmetry means that the part is invariant under all rotations about a central axis.

2 RELATED WORK

An object is symmetrical if it is invariant under geometric transformations such as *reflection*, *rotation*, *translation*, or *combinations* of these [16]. Symmetry is studied in mathematics in the scope of group theory, where it is assumed that the symmetry properties of the system are self-evident and that there is instant recognition of the symmetry group of the problem by the expert [29]. However, for systems with high-order symmetry or complex geometry, symmetry recognition by the expert may become very difficult to perform [1]. Therefore, computer-aided symmetry detection techniques have received considerable attention in different fields such as mechanical engineering [17], computer engineering [21], medicine [5], architecture and civil engineering [28]. In mechanical engineering, symmetry detection has been exploited for retrieval [2], compression [25], and alignment [3][26] of 3D CAD models, design for assembly [19], and for detecting design intent in scanned models from reverse engineering [18].

Computer-aided SD techniques can be classified according to different criteria: in terms of input data – *discrete* [7] vs *continuous* [16]-[19], in terms of scale – *global* [7]-[12][16]-[19] vs *partial* (or *quasi-symmetry*) [17][19][27] vs *local* [16][17], in terms of accuracy – *exact* (perfect)[12][16]-[19] vs *approximate* (imperfect)[7][17], in terms of distance metrics – *extrinsic* [16]-[19] vs *intrinsic* [8]. Extrinsic symmetry most often uses Euclidean distance between points to

measure the symmetry, while intrinsic symmetry is measured by different metrics such as geodesic [8]. In terms of the geometric transformation type, SD techniques may be classified into: *reflection* [16]-[19], *rotational (axisymmetry)* [16]-[19] and *cyclic* [27] symmetry), *dihedral* [1] (combination of reflection and rotational symmetry), etc. This paper focuses on exact symmetry because the accuracy of the symmetry detection needs to be at least within the manufacturing process of mechanical parts (10^{-6} m) [17]. Further, the objective is to detect global reflection and axisymmetry (see Figure 1), which are the two most common types of symmetry in mechanical engineering [14][15].

Generally, the approaches related to symmetry detection in 3D digital objects can be divided into *geometry-based* and *view-based* [15]. The *geometry-based* approach uses the geometrical information of 3D objects as input. For that purpose, different kind of 3D objects are used such as solid CAD models [16]-[19], cable-strut structures [1][29], voxel models [6], NURBS models [2][3], point clouds [9][11], mesh models [10], etc. The geometry-based approach address the detection of approximate [2][3][6][9][11] as well as exact symmetry [1][16]-[19][29]. The geometry-based approach can be further divided into those which use the local surface information [16]-[19] (e.g., surface normal, Gaussian curvature) and those which do not use it [8]-[11]. In some cases, the initial input models may be further processed and converted. For instance, mesh models were converted into voxel models [6] or point clouds [11]. The common strategy of geometry-based techniques is first to identify a larger number of candidates for the plane of symmetry (POS) or the axis of symmetry (AOS) for the given input model. The candidates are then evaluated with respect to the input geometry to determine if some of them also represent the true POS or AOS. The POS/AOS candidates were obtained by principal component analysis [8], pair matching [19], from the intrinsic surface properties [17]. Some of the proposed techniques [1][29] are constrained only to detect planes that pass through a reference point (e.g., origin, centroid, the center of mass), which is not appropriate for handling objects with weaker symmetries [9]. In the *view-based* approach, the 3D object is converted into a 2D representation such as an image [7] or a projected view [15]. The view-based approach addresses the detection of approximate symmetry and is therefore not appropriate for its implementation in mechanical parts, where the goal is to obtain exact symmetry. The 3D objects that are the scope of interest in this paper are 3D CAD models.

The symmetry detection in 3D CAD models has been studied from two aspects: *feature* and *B-rep*. The first aspect uses design features, Boolean operations, and the feature (history) tree for the detection of exact reflection and axisymmetry in parts [12] [13] and assemblies [14]. However, this aspect is restricted to native CAD models and may be sensitive to the designer's bad modeling habits. Some examples of bad modeling habits are redundant feature modeling and modeling of symmetric shapes using non-symmetric features. The second aspect uses geometry and topology information of the B-rep [16]-[19] as input, which enables using native CAD models as well as neutral exchange files for symmetry detection. To identify global reflection and axisymmetry in B-rep CAD models, the study [19] proposed a loop-based approach (a loop is a closed circuit of edges bounding a face). The approach used loop properties (e.g., loop area, centroid, normal, and so on) and a pairing algorithm to identify identical loop pairs. The candidates for the POS and AOS were calculated as the resultant vector of two-unit normal vectors from identical loop pairs. Then the candidates were ranked according to cumulative loop area and compared to extract the final POS and AOS. Another research [17] proposed a divide-and-conquer approach for detecting exact and partial global reflection and axisymmetry in B-rep CAD models, using faces as input. First, in the divide phase, the candidates for the POS/AOS were obtained through the local symmetry properties of the faces and their intersections. Then, in the conquer phase, the local symmetry properties were propagated to the global level by matching coincident local POS/AOS candidates into global POS/AOS. To reduce the meshing complexity in CAE, the study in [27] proposed an approach for detecting cyclic regions in quasi-axisymmetric B-rep CAD models using manually assigned AOS as input. Further, in [2], a graph-based approach was used to extract multi-scale (i.e., at different geometric scales) symmetric regions and extract symmetry relations among these regions. The proposed approach addressed exact reflection, rotational, and translational symmetry.

Generally, the proposed SD approaches related to B-rep CAD models have two main drawbacks: (1) they are computationally complex, mainly due to the high number of POS and AOS candidates, and are therefore not suitable for practical application (especially if the number of input models is large) (2) they are restricted to analytical geometry, i.e., up to five basic types of analytical surfaces: plane, cylinder, cone, sphere, and torus (Figure 2). However, in practice, B-rep CAD models are often a mix of analytical and numerical geometry [24]. The present paper introduces an approach that addresses both drawbacks.

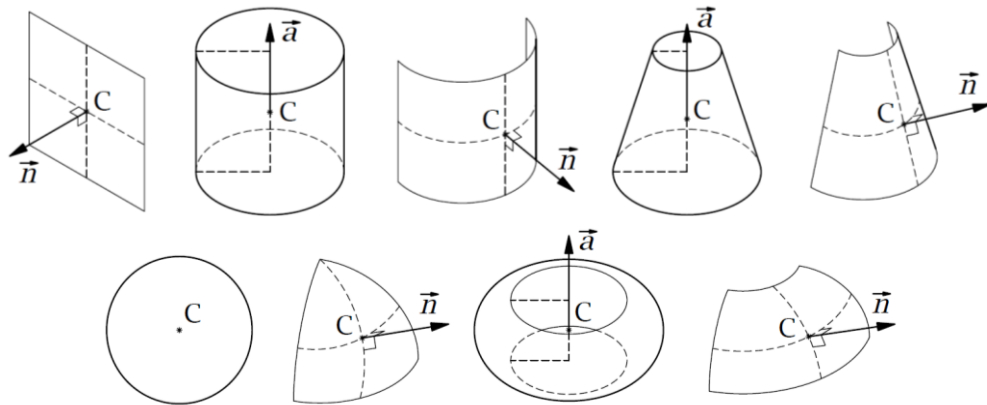


Figure 2: Different types of analytical surfaces (from top left to bottom right): (a) Plane (b) Cylinder, (c) Partial cylinder, (d) Cone, (e) Partial cone, (f) Sphere, (g) Partial sphere, (h) Torus, (i) Partial torus.

When it comes to state-of-the-art CAD systems, to our knowledge, only one offers a tool for SD. The *Symmetry check* tool [23] examines the existence of reflection symmetry in a part or assembly and identifies symmetrical, asymmetrical, and unique faces or parts using different coloring. Based on our testing performed on several CAD models, the tool seems to have no restrictions on analytical and numerical surfaces in the SD process. However, the tool also has several disadvantages: only reflection symmetry can be checked, the POS candidate needs to be manually assigned by the user, and it is not possible to check more than one POS candidate simultaneously.

3 AN APPROACH FOR COMPUTER-AIDED SYMMETRY DETECTION

The present research is motivated by the lack of relevant SD tools in state-of-the-art CAD systems and by the limitations of existing SD approaches from the research community. It was already emphasized that the prior approaches related to symmetry detection in B-rep CAD models are limited to analytical surfaces. However, in practice, the 3D CAD model also contains numerical surfaces, so the prior approaches will fail to detect symmetry.

Our approach also uses the B-Rep as input for the symmetry detection process. Most state-of-the-art CAD systems use the B-rep to describe the final shape of solids [24]. The B-rep data structure consists of topology, which defines the structure of the model, and geometry, which defines the shape of the model. The basic topological elements are faces, edges, and vertices, while the geometry consists of surfaces, curves, and points. A face is a trimmed surface, and the edge is the boundary of the trimmed surface. The B-rep data structure might also contain other topological elements such as loops, shells, co-edges, and so on. For example, a loop is a closed circuit of edges bounding a face, while a shell is a closed set of faces. The B-Rep data structure depends on the CAD system and the geometric modeling kernel it uses. CAD systems with the same geometric modeling kernel are likely to have a similar, if not identical, data structure.

The geometry in CAD systems is usually of two types: analytical and numerical [24]. Within the analytical geometry, the shape information is explicit. In contrast, within numeric geometry, the shape is controlled by the position of a set of points called control points (additionally, there can be weights and knot points in more advanced forms) [24]. The CAD system may create numerical geometry automatically in the background or intentionally by the user. For instance, when fillet or chamfer features are used to round off or break edges, the CAD system may automatically create a *blend surface* or a *B-spline surface* (Figure 3). The blend surface is transformed into a B-spline surface after exporting a native CAD model into a STEP file. In some CAD systems, the blend surface has no exact representations and is therefore approximated by the B-spline surface.

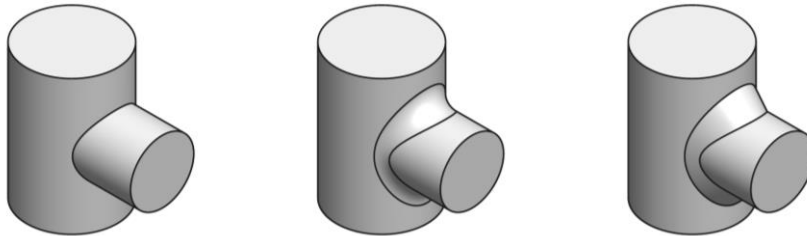


Figure 3: A test with two cylinders (left) with different diameters shows what happens if a fillet feature (middle) or chamfer feature (right) is being applied to their intersection edge. As a result, the CAD system may create numerical geometry: a blend surface (middle) and a B-spline surface (right).

In some circumstances, the user needs to create numerical geometry (such as Bézier, B-Spline, NURBS, etc.) on purpose, for instance, to model the airplane's fuselage or wing, car body, turbine blade, or any other products with a complex aesthetic shape. Another important surface is the *revolved surface* or *surface of revolution*, which is created by rotating a curve (e.g., spline) around an axis of rotation. The present paper proposes an approach that includes (apart from the five basic analytical surfaces in Figure 2) also the blend surface, B-spline surface, and the surface of revolution in the symmetry detection process (Figure 4).

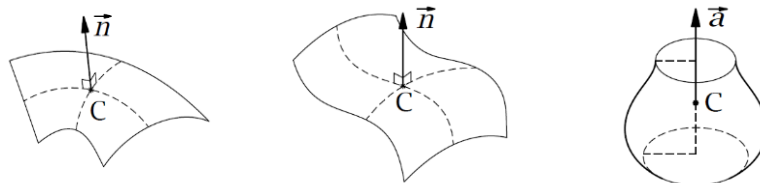


Figure 4: Different types of numerical surfaces (from left to right): (a) Blend surface, (b) B-Spline surface, and (c) Surface of revolution.

The proposed SD approach incorporates four basic steps (Figure 5):

- STEP 1 – *Identification* of the candidates for the POS and AOS,
- STEP 2 – *Classification* of all B-rep faces according to different types of surfaces,
- STEP 3 – *Evaluation* of the classified faces with respect to the POS or AOS candidates, &
- STEP 4 – *Visualization* of the detected POS or AOS in the 3D modeling space.

In the first step, the POS/AOS candidates are identified using the center of gravity and principal axis of inertia. The second step includes the classification of surfaces based on the type and the retrieval of their properties. Then, a vector-based approach and face centroids are used in the evaluation step to detect symmetry. Finally, the symmetry detection ends with the visualization step, where the symmetry information is provided to the user.

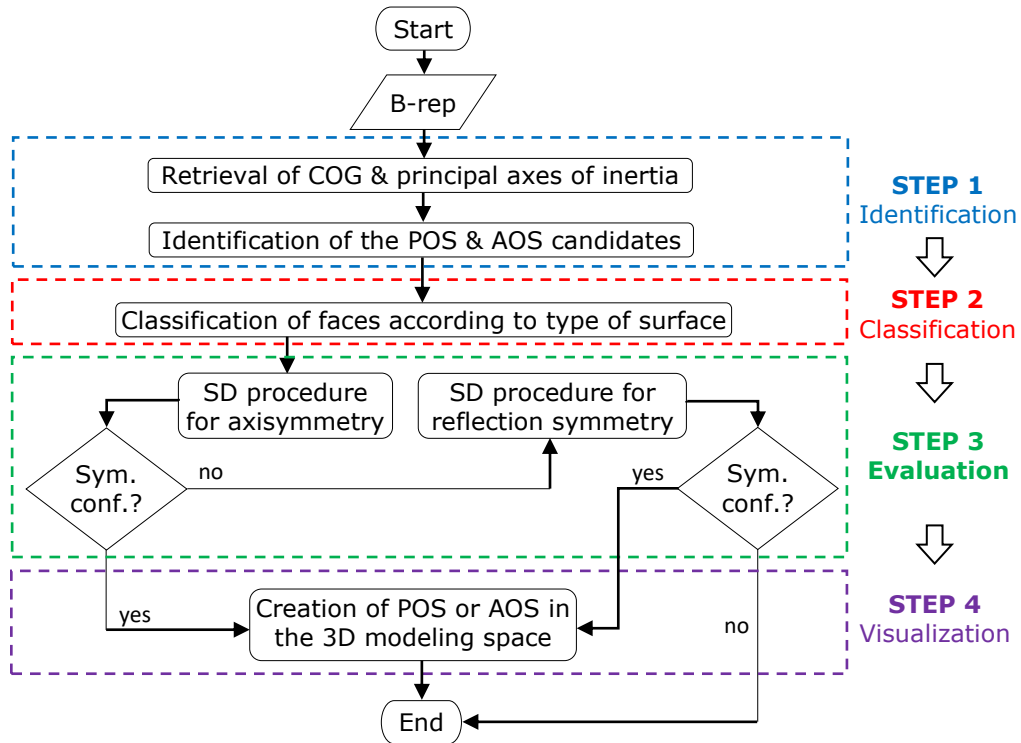


Figure 5: Flowchart of the proposed symmetry detection approach.

3.1 Step 1 – Identification

The main goal of the first step is to identify candidates for the POS and AOS. Mechanical parts usually have up to three reflection POS and one AOS (Figure 1). If the 3D model exhibits exact symmetry, then the POS and AOS must pass through its center of gravity (COG) [19]. This property can be exploited to detect exact symmetry in CAD models. For uniform density throughout the object, the center of mass and center of gravity corresponds, in fact, to the volume centroid. For a volume of arbitrary shape, the coordinates of the centroid (x_c , y_c , z_c) are defined by the following equations:

$$x_c = \frac{\int x \cdot dV}{\int dV}; y_c = \frac{\int y \cdot dV}{\int dV}; z_c = \frac{\int z \cdot dV}{\int dV} \quad (2.1)$$

where the x , y , and z terms inside the integrals denote the distances measured from the reference axes to the centroid of the differential volume. The computation of the COG (or center of mass as referred to in some CAD systems) is a standard mass property available in many state-of-the-art CAD systems.

Although the POS/AOS must pass through the 3D model's COG, their orientation will depend on the geometric shape of the 3D model. In most cases in practice, the POS will be parallel with the XY , YZ , and ZX planes of the coordinate system, while the AOS will be parallel with the axes of the coordinate system. This is because CAD systems provide default built-in planes (e.g., front, top, and right) that the designer uses for modeling purposes. However, in practice, the 3D model may still be misaligned with respect to the coordinate system of the modeling space when for instance, the base feature has a regular shape rotated with respect to the coordinate axes or an irregular shape. Hence, to overcome this misalignment issue, the present research takes

advantage of two other properties. First, if an object exhibits exact reflection symmetry, then the direction normal to the plane of symmetry is a principal axis. Second, if an object exhibits exact axisymmetry, then the axis of symmetry is a principal axis. This means that in the case of exact symmetry, the POS and AOS will be aligned with the 3D model's principal axes of inertia. Hence, the task of finding the POS/AOS orientation is turned into finding the principal axis of inertia. For that purpose, first, the moments of inertia and products of inertia need to be calculated using the following equations:

$$\begin{aligned} I_{xx} &= \int (y^2 + z^2) dm & I_{xy} &= \int (xy) dm \\ I_{yy} &= \int (z^2 + x^2) dm & I_{yz} &= \int (yz) dm \\ I_{zz} &= \int (x^2 + y^2) dm & I_{zx} &= \int (zx) dm \end{aligned} \quad (2.2)$$

Then, the inertia tensor is defined as:

$$\tilde{\mathbf{I}} = \begin{bmatrix} I_{xx} & -I_{xy} & -I_{xz} \\ -I_{xy} & I_{yy} & -I_{yz} \\ -I_{xz} & -I_{yz} & I_{zz} \end{bmatrix} \quad (2.3)$$

The angular momentum vector \mathbf{L} is proportional to the inertia tensor and angular velocity vector $\boldsymbol{\omega}$:

$$\mathbf{L} = \tilde{\mathbf{I}} \boldsymbol{\omega} \quad (2.4)$$

To find the axis of rotation where \mathbf{L} and $\boldsymbol{\omega}$ are parallel, the equation above can further be written:

$$\tilde{\mathbf{I}} \boldsymbol{\omega} = \lambda \boldsymbol{\omega} \quad (2.5)$$

Finally, the task of finding the principal axis of inertia becomes an eigenvalue problem:

$$|\tilde{\mathbf{I}} - \lambda \mathbf{I}| = 0 \quad (2.6)$$

From the equation above, the three eigenvalues are the principal moments of inertia, and the three eigenvectors are the principal axis of inertia. Generally, the 3D model's principal axes of inertia are, in the same way as the COG, a standard mass property available in many CAD systems. Finally, the candidates for the POS are defined by the plane equation:

$$\frac{a}{(x - x_c)} + \frac{b}{(y - y_c)} + \frac{c}{(z - z_c)} = 0 \quad (2.7)$$

while the AOS candidates are defined by the line equation:

$$\frac{(x - x_c)}{a} = \frac{(y - y_c)}{b} = \frac{(z - z_c)}{c} \quad (2.8)$$

where the variables a , b , and c represent the components of the principal axis, while x_c , y_c , and z_c are the coordinates of the COG. Since there are three candidates for the POS and AOS, there will also be three equations of (2.7) and (2.8).

3.2 Step 2 – Classification

In the classification step, each face of the B-rep model is classified based on the type of its underlying surface (Figure 2 and Figure 3): plane, cylinder, partial cylinder, cone, partial cone, sphere, partial sphere, torus, partial torus, blend surface, surface of revolution, and B-spline surface. Each face of the model is marked with a unique name (e.g., planes with PL1, PL2, PL3, PL4, ..., cylinders with CY1, CY2, CY3, CY4, ..., cones with CO1, CO2, CO3, CO4, ..., and so on), to enable its tracking and accessibility at any time. In addition, the properties for each face, such as the surface area, perimeter, face centroid, face normal, edge count, loop count, vertex count, etc., are retrieved. The properties are used as criteria to identify identical face pairs in the next step. If the 3D model's COG is not coincident with the coordinate system's origin in the modeling space,

the whole 3D model will be mathematically translated into it. Finally, all faces, including their related properties, are stored for the next step. Generally, the classification step is necessary because only surfaces of the same class will be later compared in the evaluation phase.

3.3 Step 3 – Evaluation

In the third step, the classified faces are evaluated with respect to the POS and AOS candidates. For that, two evaluation procedures are used, one for reflection and the other for axisymmetry. The *evaluation procedure for reflection symmetry* relies on pairwise comparison, where all faces from the same class are mutually compared based on their properties to identify symmetric face pairs. For that purpose, the *centroid vector* and the *unit normal vector* or the *unit axis vector* are created for each face (see Figure 2). The *centroid vector* is defined by the initial point (the COG) and the terminal point (the face centroid). The *unit normal vector* or *unit axis vector* are extracted at the face centroid. The face centroid C is the geometric center of the underlying surface (see Figure 2). Two faces are reflective symmetric if they fulfill the following criteria: *equality*, *equidistance*, and *direction*. The fulfillment of the *equality* criterion means that two faces have the same values of the following properties: surface area, perimeter, number of edges, loops, and vertices. The *equidistance* criterion is satisfied if two face centroids are equally distanced from the POS, i.e., the magnitudes of their centroid vectors are equal. In addition, the resultant vector of the two centroid vectors is calculated, and the component normal to the POS candidate must be zero. The last criterion, *direction*, is met when two corresponding face unit normal vectors have opposite directions with respect to the POS candidate. All faces which do not belong to some symmetry pair must satisfy the condition that their centroid lies on the POS candidate, which is queried with equation (2.3). An illustrative example of the procedure for reflection symmetry is shown in Figure 6.

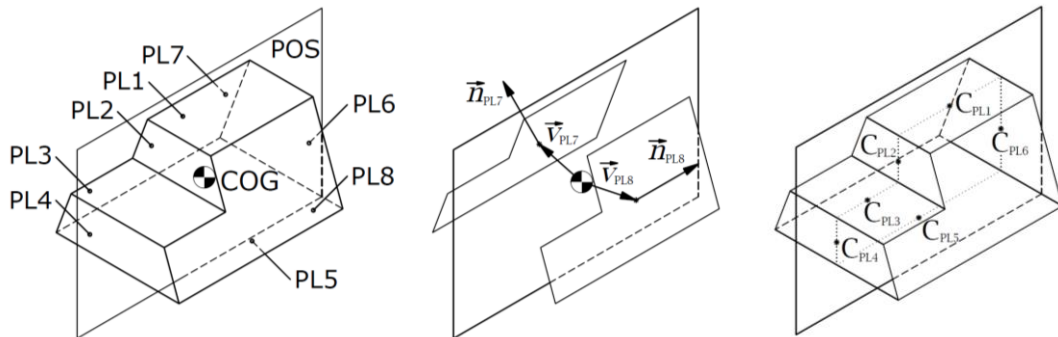


Figure 6: An example of a reflective symmetric object with eight planar faces, its COG, and the POS candidate (left figure). The middle figure shows the centroid vectors and unit normal vectors of the symmetric face pair PL7 and PL8. The right figure shows the remaining faces PL1-PL6 with their face centroids lying on the POS.

Finally, a 3D model exhibits reflection symmetry with respect to the POS candidates only if it satisfies the equilibrium equation for reflection symmetry: the sum of symmetric face pairs f_p and individual faces f_c whose centroids lie on the POS candidate equals the total number of faces n in the 3D model:

$$\sum f_p + \sum f_c = n \quad (3.1)$$

The *evaluation procedure for axisymmetry* is slightly simpler than the reflection symmetry procedure. A face is axisymmetric with respect to the AOS candidate if it fulfills the following two criteria: *coincident* and *direction* (see Figure 7). The *coincident* criterion is fulfilled if the AOS candidate lies on the face centroid, which is queried with Equation (2.8). The *direction* criterion is satisfied if either the *unit normal vector* or the *unit axis vector* of the face has the same direction

as the AOS candidate. Finally, the 3D model exhibits axisymmetry if the equilibrium equation for axisymmetry is met, i.e., the sum of all faces that fulfill the two criteria is equal to the total number of faces n in the 3D model:

$$\sum f_c = n \quad (3.2)$$

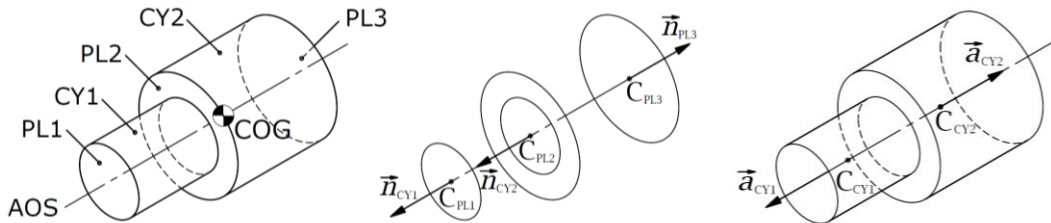


Figure 7: An example of an axisymmetric object with three planar and two cylindrical faces, its COG, and the AOS candidate (left figure). The middle figure shows planar faces PL1, PL2, and PL3 with their centroids lying on the AOS and the unit normal vectors pointing in the direction of the AOS. The right figure shows the remaining cylindrical faces CY1 and CY2 with their face centroids lying on the AOS and unit axis vectors pointing in the direction of the AOS.

3.4 Step 4 – Visualization

In the last step, if reflection or axisymmetry has been confirmed in the 3D model using the equilibrium equations (3.1) and (3.2), the corresponding POS or AOS will be visualized in the 3D modeling space, thus providing the user the information about the symmetry. Generally, to create a plane in Euclidean space, a unit normal vector and a point through which it is passing is required. Hence, the POS is created using the principal axis of inertia and the COG. On the other hand, to generate an axis in Euclidean space, the unit axis vector and the point through which it is passing are necessary. Thus, the AOS is created by means of the principal axis of inertia and COG.

4 IMPLEMENTATION

The proposed SD approach was implemented into the commercial CAD system Solidworks 2020 using its Application Programming Interface (API). It is essential to highlight that the CAD system has only been exploited as a tool for implementing of the SD approach and that any other CAD system API could have been used for that purpose as well. One of the main advantages of the Solidworks API compared to other CAD systems is the possibility to access the complete API object hierarchy even with the low-level programming languages, making it suitable for implementing the proposed symmetry detection approach. The SD approach has been implemented at the macro level using the Visual Basic for Application (VBA) programming language. The disadvantage of macros is that they are slower compared to Add-ins or Stand-alone Applications because they do not run on their own memory space. However, macros are easy to implement and can be developed in a reasonable time frame.

All steps were implemented in the order described in the previous section. First, the 3D model's COG and the principal axes of inertia are retrieved from the CAD system to identify the POS and AOS candidates. Then all faces from the 3D model are looped for classification and storing in an array. After that, all faces from the same class are looped to identify individual faces whose centroids pass through the POS or AOS and to conduct the pairwise comparison process to identify symmetric face pairs. During the evaluation process, first, the axisymmetry procedure is performed. In case axisymmetry has been confirmed, the visualization step will proceed, otherwise the procedure for reflection symmetry will further proceed (see Figure 5). The corresponding POS will be visualized in the 3D modeling space if reflection symmetry has been detected.

5 VALIDATION

The implemented SD approach has been validated on a representative sample of 100 CAD models exhibiting reflection symmetry, and on 50 axisymmetric CAD models (an illustrative example of the test parts is shown in Figure 8). The CAD models were collected from the industry and are CNC-milled and turned mechanical parts. The share of the surfaces in the tested parts was as follows: 43.4% planes, 29.5% cylinders, 9.5% cones, 4.9% spheres, 5.9% tori, 1.5% surface of revolution, 2.9% blend surfaces, and 2.4% B-spline surfaces.

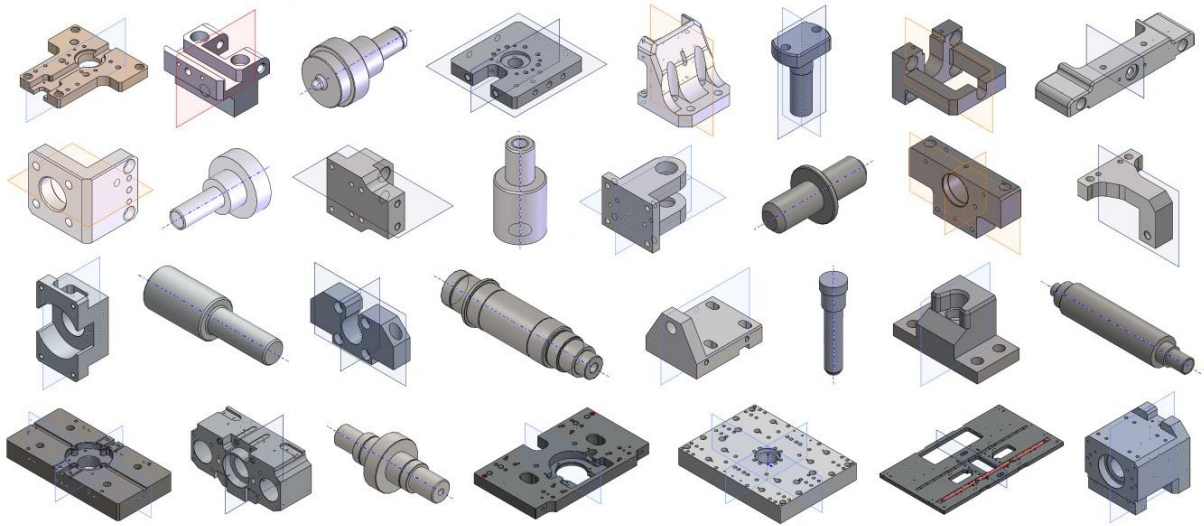


Figure 8: An example of the test CAD models with the detected plane(s) or axis of symmetry.

The testing was conducted on native CAD models and neutral STEP files (exported from the native models and imported back into the CAD system). The primary scope of the testing was to validate the *accuracy* and *computational complexity* of the proposed SD approach. The accuracy represents the correctness of the symmetry detection process, i.e., the correctness of detecting the corresponding POS and AOS. The computational complexity was evaluated using Big-O complexity charts. Additionally, the testing was exploited to reveal any computational errors and technical issues. The testing was performed on a Dell Precision Working station with Intel i7-1165G7 up to 4.7 GHz processor and 16 GB RAM.

The accuracy of the automatically detected POS and AOS has been evaluated manually by experts. Figure 7 illustrates the detected POS and AOS in some tested parts. The test results show that the proposed SD approach enables accurate detection of the POS in 97% of test cases. In only 3% of test cases, the proposed SD approach has not recognized the existing reflection symmetries (Figure 9). In some rare cases, incomplete symmetry detection may occur in mechanical parts with multiple reflective symmetries (usually more than three) and is caused when the POS is misaligned with the principal axes of inertia. On the other side, the corresponding AOS has been recognized in all test parts, so the detection accuracy for axisymmetry is 100%.

For estimation of the computational complexity, the Big-O complexity chart is used, which represents the computational complexity expressed as a function of the size of the input n . In our case, the input n is the number of faces in the tested B-rep CAD models. The theoretical computational complexity has been estimated as follows. Steps 1 and 4 do not depend on the input n and have constant time $O(1)$. Step 2 performs a looping operation of the entire input n and requires $O(n)$ time, while the pairwise comparison process in Step 3 results in $O(n^2)$ time. On the other hand, the empirical computational complexity has also been estimated (Figure 10).

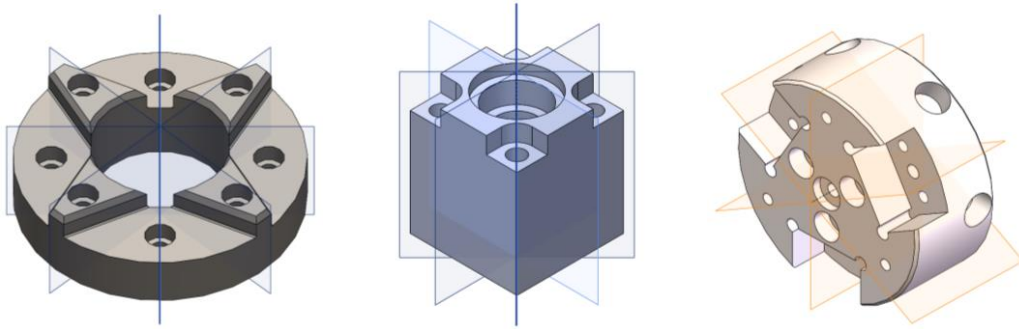


Figure 9: Incomplete symmetry detection in mechanical parts exhibiting multiple reflection symmetries. In 3% of test cases, the proposed symmetry detection approach cannot detect the existing reflection symmetries. Two parts (left and middle) had four POS, while only two of them have been detected. Another part (right) had three POS, but only one has been detected.

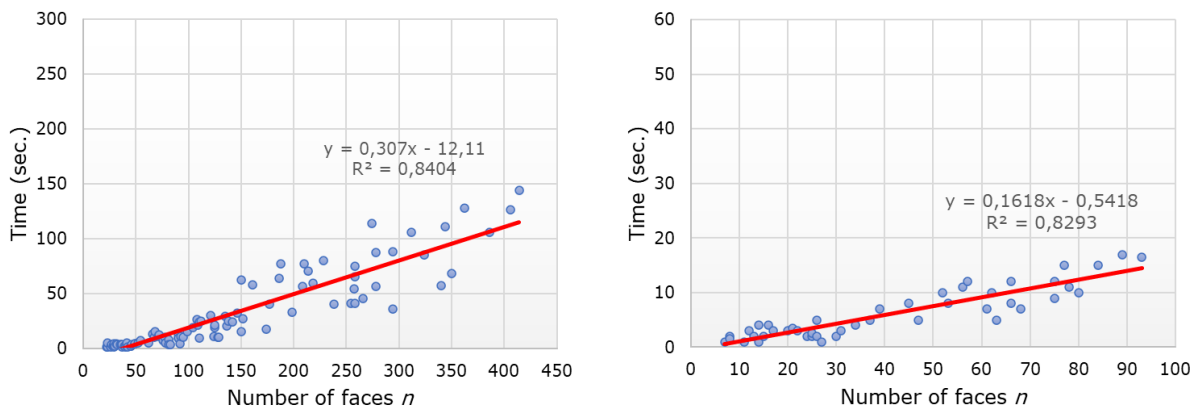


Figure 10: Big-O complexity charts for reflection symmetry (left) and axisymmetry (right) expressed as the size of the input n (i.e., the number of faces).

The empirical computational complexity was evaluated by testing all CAD models on the same hardware, and the symmetry detection running time (in seconds) was measured for each CAD model. Based on that, two computational complexity charts were created, one for reflection symmetry and the other for axisymmetry (Figure 10). The Big-O complexity chart for detecting reflection symmetry and axisymmetry shows that the empirical computational complexity is $O(n)$, which is less than the theoretical computational complexity of $O(n^2)$. An explanation for this might be that the input size n needs to be significantly bigger to show the quadratic trend of the computational complexity. Another reason might be the nature of the representative CAD models, which are namely composed of different surface types, so the actual number of pairwise comparisons is lower than the total number of faces n . The theoretical number of pairwise comparisons would correspond to the case if the 3D model was mad-up of only the same surface type (e.g., planar), which is seldom the case in practice. Our approach is more efficient when comparing our results with another approach for symmetry detection in B-rep models [19], where the computational complexity was estimated to be $O(n^4)$.

6 LIMITATIONS

The proposed SD approach is limited to single parts with a single body and does not apply assembly models. It is focused on detecting reflection and axisymmetry, although mechanical parts

may also exhibit cyclic symmetry. The blend surfaces and B-spline surface are not likely to occur in CAD models exhibiting axisymmetry and were therefore only included in the SD procedure for reflection symmetry. The surface of revolution was considered for both SD procedures (this is important because the torus surface from the native CAD models is transformed into a surface of revolution after exporting it to the STEP file). Further, the proposed SD approach cannot handle periodical surfaces (e.g., cylinders, cones, etc.) that are split into two halves (this is characteristic of CATIA V5 CAD models). Finally, the proposed SD approach works for CAD models with exact symmetry where the POS or AOS are aligned with the principal axes. Therefore, it is not applicable for CAD models exhibiting partial symmetry.

7 CONCLUSIONS AND FUTURE WORK

This paper proposes an approach for computer-aided symmetry detection of exact global reflection and axisymmetry in B-rep CAD models. What distinguishes our symmetry detection approach from the prior is that it is not restricted to only five analytical surfaces (plane, cylinder, cone, sphere, and torus), but it can also handle numerical surfaces (blend surface, B-spline surface, and surface of revolution). The approach was implemented into a state-of-the-art CAD system for validation purposes. The validation was performed through the testing of 3D CAD models collected from the industry. It was confirmed that the approach enables accurate detection of the planes of symmetry in 97% of the tested cases and the axes of symmetry in 100% of the tested cases. The empirical computational complexity of our symmetry detection approach was evaluated to be $O(n)$. The future research will be focused on the following points: (i) extending the testing to a larger number of CAD models and other types of mechanical parts (e.g., sheet metal, forged, cast, etc.), (ii) overcoming incomplete symmetry detection in parts exhibiting multiple reflective symmetries by extending the number of POS candidates, (iii) extending the SD approach for the detection of cyclic and partial symmetry, and (iv) improving the SD approach for handling periodical surfaces (e.g., cylinders) that are split into two halves.

ACKNOWLEDGEMENT

This paper reports on work funded by the Croatian Science Foundation project IP-2018-01-7269: Team Adaptability for Innovation-Oriented Product Development - TAIDE.

Mladen Buric, <http://orcid.org/0000-0001-8921-6024>

Mario Brcic, <https://orcid.org/0000-0002-7564-6805>

Nenad Bojcetic, <https://orcid.org/0000-0001-7353-0537>

Stanko Skec, <https://orcid.org/0000-0001-7549-8972>

REFERENCES

- [1] Chen; Y.; Linzi, F.; Feng, J.: Automatic and Exact Symmetry Recognition of Structures Exhibiting High-Order Symmetries, *Journal of Computing in Civil Engineering*, 32(2), 2018. [https://doi.org/10.1061/\(ASCE\)CP.1943-5487.0000743](https://doi.org/10.1061/(ASCE)CP.1943-5487.0000743)
- [2] Dang, Q.; Morin G.; Mouysset S.: Symmetry and Fourier Descriptor: A Hybrid Feature For NURBS based B-Rep Models Retrieval. Conference: Eurographics Workshop on 3D Object Retrieval, 2014, 45-52. <http://dx.doi.org/10.2312/3dor.20141049>
- [3] Dang, Q.; Mouysset S.; Morin G.: Symmetry-Based Alignment for 3D Model Retrieval, 12th International Workshop on Content-Based Multimedia Indexing (CBMI), 2014, pp. 1-6, <https://doi.org/10.1109/CBMI.2014.6849816>
- [4] Deng, X.; Wang, J.: Research on the manufacturing of mechanical parts based on the theory of space symmetry group, *Academic Journal of Manufacturing Engineering* 15(1), 2017, 64-71.

- [5] Fotouhi, J.; Taylor, G.; Unberath, M.; Johnson, A.; Lee, S.C.; Osgood, G.; Navab N. Exploring Partial Intrinsic and Extrinsic Symmetry in 3D Medical Imaging, *Medical Image Analysis*, 2020, <https://doi.org/10.48550/arXiv.2003.02294>
- [6] Gao, L.; Zhang, L.; Meng, H.; Ren, Y.-H.; Lai, Y.-K.; Kobbelt, L.: PRS-Net: Planar Reflective Symmetry Detection Net for 3D, *IEEE Transactions on Visualization and Computer Graphics*, 27(6), 2021, 3007-3018. <https://doi.org/10.1109/TVCG.2020.300382>
- [7] Gothandaraman, R.; Jha, R.; Muthuswamy, S.: Reflectional and rotational symmetry detection of CAD models based on point cloud processing, *IEEE 4th Conference on Information & Communication Technology (CICT)*, Chennai, India, 2020, 1-5. <https://doi.org/10.1109/CICT51604.2020.9312109>
- [8] He, C.; Wang L.; Zhang Y.; Wang, C.: Dominant Symmetry Plane Detection for Point-Based 3D Models, *Advances in Multimedia*, 5, 2020, 1-8. <https://doi.org/10.1155/2020/8861367>
- [9] Hruda, L.; Kolingerová, I.; Váša, L.: Robust, fast and flexible symmetry plane detection based on differentiable symmetry measure, *The Visual Computer*, 38(24), 2022, 555-571. <https://doi.org/10.1007/s00371-020-02034-w>
- [10] Hruda, L.; Dvorak, J.: Estimating Approximate Plane of Symmetry of 3D Triangle Meshes, *Proceedings of CESC 2017: The 21st Central European Seminar on Computer Graphics*, 2017.
- [11] Ji, P.; Liu, X.: A fast and efficient 3D reflection symmetry detector based on neural networks, *Multimedia Tools and Applications*, 78, 2019, 35471-35492. <https://doi.org/10.1007/s11042-019-08043-9>
- [12] Jiang J.; Chen Z.; He K.: A feature-based method of rapidly detecting global exact symmetries in CAD models, *Computer-Aided Design*, 45, 2013, 1081-1094. <https://doi.org/10.1016/j.cad.2013.04.005>
- [13] Jiang, J.; Chen Z.; He, K.: A feature-based approach for detecting global symmetries in CAD models with free-form surfaces, *13th International Conference on Computer-Aided Design and Computer Graphics*, 2013, [10.1109/CADGraphics.2013.58](https://doi.org/10.1109/CADGraphics.2013.58)
- [14] Jiang, J.; Gong, Q.; Chen, Z.; He, K.; Ruang, R.: A Feature-based Method of Rapidly Detecting Global Symmetries of Static Assembly CAD Models, *Jisuanji Fuzhu Sheji Yu Tuxingxue Xuebao/Journal of Computer-Aided Design and Computer Graphics*, 29(5), 2017, 950-957.
- [15] Li, B.; Johan, H.; Ye, Y.; Lu, Y.: Efficient 3D reflection symmetry detection: A view-based approach, *Graphical Models*, 83, 2016, 2-14. <https://doi.org/10.1016/j.gmod.2015.09.003>
- [16] Li, C.; Li, M.; Gao, S.: Multi-scale symmetry detection of CAD models, *Computer-Aided Design and Applications*, 16(1), 2018, 50-66. <https://doi.org/10.14733/cadaps.2019.50-66>
- [17] Li, K.; Foucault G.; Léon J.; Trlin, M.: Fast global and partial reflective symmetry analyses using boundary surfaces of mechanical, 53, 2014, 70-89. <https://doi.org/10.1016/j.cad.2014.03.005>
- [18] Li, M.; Langbein, F.; Martin, R.: Detecting design intent in approximate CAD models using symmetry. *Computer-Aided Design*, 42, 2010, 183-201. <https://doi.org/10.1016/j.cad.2009.10.001>
- [19] Tate, S.; Jared, G.: Recognizing symmetry in solid models, 35(7), 2003, 673-692. [https://doi.org/10.1016/S0010-4485\(02\)00093-3](https://doi.org/10.1016/S0010-4485(02)00093-3)
- [20] Ma, Z.; Zhang, T; Liu, F.; Yang J.: Knowledge discovery in design instances of mechanical structure symmetry, *Advances in Mechanical Engineering*, 7(11), 2015, 1-19. <https://doi.org/10.1177/1687814015615044>
- [21] Nagar, R.; Raman S.: 3DSymm: Robust and Accurate 3D Reflection Symmetry Detection, *Pattern Recognition*, 107(5):107483, 2020, <https://doi.org/10.1016/j.patcoq.2020.107483>
- [22] Simmons, C. H.; Phelps, N.: *Manual of Engineering Drawing Technical Product Specification and Documentation to British and International Standards*, Fourth Edition, ISBN: 978-0-08-096652-6, Butterworth-Heinemann, 2012.
- [23] Solidworks 2020 Help, <http://help.solidworks.com/>

- [24] Stroud, I.; Nagy, H.: Solid modelling and CAD systems: How to survive a CAD system, Springer, London., 2011. <https://doi.org/10.1007/978-0-85729-259-9>
- [25] Tayangkanon, T.; Sompagdee, P.; Li, X.: 3D Model Compression over ASCII Encoded Using Rotational and Reflective Symmetry, 2018 10th International Conference on Knowledge and Smart Technology (KST), 2018, 53-58. <https://doi.org/10.1109/KST.2018.8426067>
- [26] Tedjokusumo, J.; Leow, W.K.: Normalization and Alignment of 3D Objects Based on Bilateral Symmetry Planes. In: Cham, T.J., Cai, J., Dorai, C., Rajan, D., Chua, T.S., Chia, L.T. (eds) Advances in Multimedia Modeling. MMM 2007. Lecture Notes in Computer Science, vol 4351. Springer, Berlin, Heidelberg, 2006. https://doi.org/10.1007/978-3-540-69423-6_8
- [27] Tierney, C.; Boussuge, F.; Robinson, T.; Nolan, D.; Armstrong, C.: Efficient symmetry-based decomposition for meshing quasi-axisymmetric assemblies, Computer-Aided Design and Applications, 16(3), 2019, 478-495. <https://doi.org/10.14733/cadaps.2019.478-495>
- [28] Xue, F.; Chen, K.; Lu, W.: Architectural Symmetry Detection from 3D Urban Point Clouds: A Derivative-Free Optimization (DFO) Approach, Advances in Informatics and Computing in Civil and Construction Engineering, 2019, 513-519. https://doi.org/10.1007/978-3-030-00220-6_61
- [29] Zingoni, A.: Symmetry recognition in group-theoretic computational schemes for complex structural systems, Computers and Structures, 94-95, 2012, 34-44. <https://doi.org/10.1016/j.compstruc.2011.12.004>